JACS
JOURNAL OF THE AMERICAN CHEMICAL SOCIETY

Article

pubs.acs.org/JACS

Chemical Probes and Engineered Constructs Reveal a Detailed Unfolding Mechanism for a Solvent-Free Multidomain Protein

Joseph D. Eschweiler, Rachel M. Martini, and Brandon T. Ruotolo*

Department of Chemistry, University of Michigan, Ann Arbor, Michigan 48109, United States

Supporting Information

ABSTRACT: Despite the growing application of gas-phase measurements in structural biology and drug discovery, the factors that govern protein stabilities and structures in a solvent-free environment are still poorly understood. Here, we examine the solvent-free unfolding pathway for a group of homologous serum albumins. Utilizing a combination of chemical probes and noncovalent reconstructions, we draw new specific conclusions regarding the unfolding of albumins in the gas phase, as well as more general inferences regarding the sensitivity of collision induced unfolding to changes in protein primary and tertiary structure. Our findings suggest that the general unfolding pathway of low charge state albumin ions is largely unaffected by changes in primary structure; however, the stabilities of intermediates along these pathways vary widely as sequences diverge. Additionally, we find that human albumin follows a domain associated unfolding pathway, and we are able to assign each unfolded form observed in our gas-phase data set to the disruption of specific domains within the protein. The totality of our data informs the first detailed mechanism for multidomain protein unfolding in the gas phase, and highlights key similarities and differences from the known solution-phase pathway.

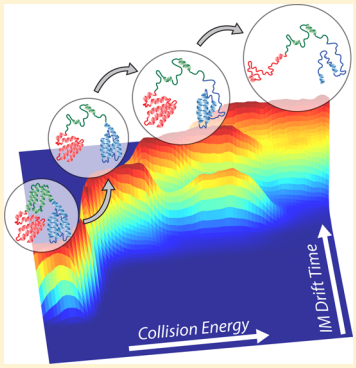

INTRODUCTION

A detailed understanding of protein structure is centrally important in the postgenomic era, especially in the context of human disease.[1] Despite nearly 60 years of molecular-level observations, and an online repository of nearly 120,000 structural data sets, our ability to predict the three-dimensional fold of an amino acid sequence *ab initio* is mainly limited to small, single domain proteins.[2] In contrast, the successes of template-based methods of protein structure prediction, relying upon previously captured structural data, can extend to much larger sequences.[3] Currently, such data sets are limited primarily to those gathered through X-ray diffraction, nuclear magnetic resonance (NMR) spectroscopy, or electron microscopy (EM).[4] While all highly enabling, high-resolution technologies in their own right, these techniques also bear significant limitations in terms of their throughput and their ability to access mixtures, thus rendering significant regions of the proteome absent from our current structural databases and refractory to rational drug design efforts.[5] Therefore, it is clear that, in order to move forward our fundamental understanding of the forces that drive environment-dependent protein folding reactions, protein structure data from other experimental methods must be considered.

Beginning with the introduction of electrospray ionization (ESI)[6] and matrix-assisted laser desorption ionization (MALDI)[7,8] over 25 years ago, solvent-free biomolecular structure has been targeted in an effort to resolve some of the mysteries surrounding native protein folding. In the gas phase, a simplified state of biological matter can be accessed, free from its native environment and accessible to high resolution spectrometric techniques. Surprisingly, many aspects of native protein structure can be retained *in vacuo*, including protein complex binding stoichiometry and topology.[9] In addition, the locations of bound substrates[10,11] and overall protein folds[12,13] can exhibit a strong memory of their native forms when observed in the gas phase. Technologies including gas-phase hydrogen−deuterium exchange mass spectrometry,[14,15] action spectroscopy,[16] and ion mobility-mass spectrometry (IM-MS)[17] have revealed that gas-phase proteins are not "inside out" as originally surmised[18] but are instead largely charge solvated, existing in multiple iso-energetic states, and can strongly resemble their native-like forms.[19]

A key observation from such gas-phase structural biology measurements is that solvent-free proteins can undergo unfolding following sufficient collisional heating, and that unfolding pathways can be monitored by IM-MS and mined for detailed structural information.[20] Generally, these experiments involve sequentially increasing the kinetic energy of ions as they enter a pressurized ion trap, and thereby collisionally heating them. Subsequent analysis of IM drift time distributions for ion populations postactivation generally reveals increases in ion collision cross sections as in a manner correlated with their increased internal energies. Although generalized correlations between gas-phase and native state protein stabilities are not yet available, gas-phase protein unfolding has already demonstrated substantial promise as a fingerprinting technology in biomolecular analysis.[21] Early IM-MS measurements revealed that

Received: November 10, 2016
Published: December 13, 2016

DOI: 10.1021/jacs.6b11678
J. Am. Chem. Soc. 2017, 139, 534−540

single domain protein ions containing disulfide bonds resist collision induced unfolding (CIU) more so than those that lack such bonding.[22] Subsequent CIU experiments targeted protein−protein and protein−ligand complexes, and highlighted the ability of gas-phase unfolding to detect minor differences in protein stability connected to changes in both local and global protein structure.[23−27] More recent experiments have discerned the ability of CIU to detect conformationally selective ligand binding,[28] the cooperative stabilization upon ligand binding in multiprotein complexes,[29] the details of disulfide bond structure within intact antibodies,[30] and a domain-correlated mechanism of gas-phase unfolding overall.[31] Despite these insights, we still lack a clear, detailed picture of protein CIU. Information regarding the extent to which gas phase unfolding mimics such processes in solution, as well as a detailed view of domain-correlated unfolding events achieved in the absence of bulk solvent, could be transformative for both CIU as an analytical tool and our ability to predict protein structure.

In this report, we use a variety of homologous serum albumins to study the sensitivity of CIU to changes in primary structure. Additionally, we utilize domain-specific chemical probes and novel noncovalent constructs to assign CIU transitions to specific regions of human serum albumin (HSA). Taken together, our results demonstrate, for the first time, a detailed mechanism of gas-phase protein unfolding that links individual increases in ion size to unfolding events within specific regions of a multidomain protein. In addition, by comparing our gas-phase results with well-known mechanisms of HSA unfolding in solution,[32] we are able to determine that elements of albumin CIU strongly resemble albumin unfolding in solution, adding further evidence of solution-phase memory in gas-phase proteins and allowing us to point toward future applications of CIU in protein stability analyses.

EXPERIMENTAL SECTION

Sample Preparation. Wild type (WT) bovine, hominian, ovine, leporine, caprine, murine, and porcine serum albumin were purchased from Sigma-Aldrich (St. Louis, MO) as lyophilized powders at purities greater than 97% (Table S1). The lyophilized proteins were diluted to 100 μM in 100 mM ammonium acetate and stored at −80 °C. 8-Anilino-1-naphthalenesulfonic acid (ANS) ammonium salt hydrate (97%), warfarin (WRF, analytical grade), indomethacin (IDM, 99%), L-thyroxine (98%), bilirubin (98%), and hemin (HMN, 98%) were also purchased from Sigma-Aldrich; 10 mM DMSO stocks were prepared prior to each experiment. A stock solution of 1 mg/mL diazepam (DZP) was generously provided by the Kennedy Group at the University of Michigan. Recombinant albumin domains 1, 2, and 3 as well as the domain 1−2 fusion protein were purchased from Albumin Biosciences (Huntsville, AL) as lyophilized powders. Recombinant albumin domains were diluted to 90 or 180 μM in 100 mM ammonium acetate and stored at −80 °C.

IM-MS Data Collection. CIU fingerprints were obtained on a Synapt G2 IM-MS instrument (Waters Corp, Manchester, U.K.) as described previously.[31] Briefly, albumin samples were diluted to 10 μM and loaded into homemade, gold coated borosilicate needles. The cone voltage was maintained at 1.5 kV with the sampling and extraction cones set to 30 and 2 V, respectively. The source pressure was set to 50 mbar, and the source backing pressure was adjusted to 9 mbar. For all measurements, the quadrupole was set to isolate the 15^+ charge state between 4420 and 4450 m/z. The IM T-wave ion guide was operated at 4 mbar with wave height and wave velocity values of 15 V and 150 m/s, respectively. Mass spectra and drift time distributions were obtained for the ions at multiple trap collision energies in steps of 2 V from 20 to 188 V. All collision cross section (CCS) values, which relate IM drift times directly to ion size and shape, were calibrated using ions of known CCS as described previously and detailed in Table S2.[33]

Chemical Probe CID Analysis. HSA was incubated with chemical probes at a ratio of 10 uM protein to 100 uM probe with a DMSO content of less than 5%. Experiments were performed as described above, although the quadrupole was adjusted to isolate either singly bound or apo protein. Selected measurements were chosen for replication, and their variabilities were found to be ±2 V, much lower than what is needed for our data analysis.

CIU/CID Analysis of Reconstituted HSA. Noncovalent reconstitutions of HSA were prepared by mixing component domains and incubating on ice for 10 min. The domain 1−2 fusion protein was incubated with domains 1, 2, and 3 at concentrations of 45 uM to provide noncovalent complexes. These complexes were then subjected to CIU and CID analysis without quadrupole selection. We similarly analyzed nonspecific trimers comprised of domains 1, 2, and 3, as well as the specific trimer of domains 1, 2, and 3.

IM-MS Data Analysis. CIU fingerprints, subsequent RMSD calculations, and feature analysis were carried out using CIUSuite.[34] CID analysis of both chemical probes and reconstituted HSA complexes was carried out using Masslynx (Waters Corp. Manchester, U.K.).

RESULTS AND DISCUSSION

Effects of Protein Primary Structure on CIU. Previous studies from our group have indicated that the CIU behavior of proteins is sensitive to their domain structure.[31] To further understand the effects of intermolecular interactions governed by primary structure on the global CIU process, we undertook analysis of seven homologous serum albumins. Each SA studied is a single polypeptide chain composed of three homologous domains (D1, D2, and D3), all of which share near-identical tertiary structure while differing significantly in primary structure from 70 to 90% sequence identity.

Previous work has revealed that the CIU fingerprint of an ion is dependent on its charge state.[31] Figure 1A shows the average unfolding pathway for seven homologous albumins for the 14, 15, and 16^+ charge states. The standard deviation plots to the right characterize the variability between these structures caused by subtle changes to primary structure. As expected, the lowest charge state, 14^+, requires higher voltages to unfold and generally accesses fewer intermediate structures along the unfolding pathway. For the 15^+ and 16^+ ions, the average behavior of the seven homologues is quite similar, giving rise to a plurality of intermediate conformer families during CIU. Interestingly, analysis of the standard deviation plots reveals significant differences in CIU response caused by small changes to primary structure. We identified the 15^+ ion not only as having the highest total deviation from the mean but also as exhibiting significant deviations across the largest area of the unfolding fingerprint. We note that standard deviation values between replicates of the same protein are generally at least 5 times lower than those reported here across homologues. Due to this potential richness of information, we chose to focus on this charge state for further analysis and discussion. The reader is directed to Figure S1 for CIU fingerprints for individual 14^+ and 16^+ homologues.

Analysis of the resulting fingerprints for 15^+ serum albumins (Figure 1G−L, Figure S2) reveals clear similarities. For example, all albumins appear to undergo the same structural transitions upon collisional activation, resulting in a total of $N+1$ conformer families, where N is the number of domains in the native structure (labeled 1−4 in Figure 1G). This behavior is predicted from our previous work, which describes a method for predicting optimal charge states for CIU analysis.[31] It

DOI: 10.1021/jacs.6b11678
J. Am. Chem. Soc. 2017, 139, 534−540

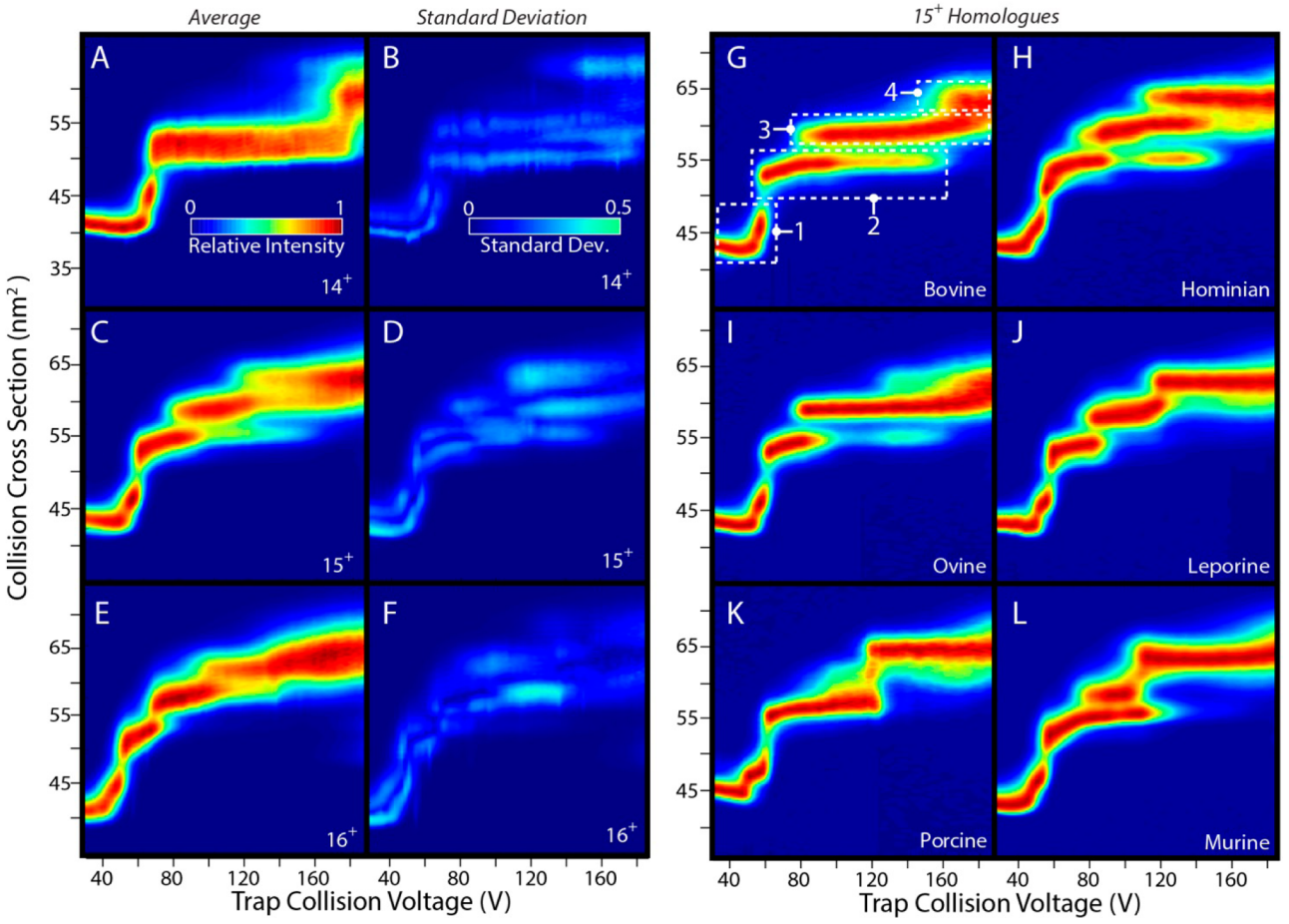

Figure 1. CIU screen of homologous serum albumins. Average and standard deviation CIU fingerprints of seven homologous serum albumins at charge states 14^+ (A, B), 15^+ (C, D), and 16^+ (E, F). Examples of albumin CIU fingerprints from various species acquired for 15^+ ions (G–L as indicated on the figure). Four main conformer families (1–4, highlighted in part G) are detected throughout.

should be noted that transitions and conformer families are assigned on the basis of their stabilities, signal intensities, and resolution in CCS/energy space (see the Supporting Information for more details on CIU feature assignments).

Further analysis using the feature extraction and characterization functions of CIUSuite revealed additional information regarding the gas-phase unfolding pathways of homologues (Tables S3–S6, Figures S3 and S4). We characterized each CIU conformer family in terms of its centroid drift time, the range of voltages over which the conformer family is stable, and the centroid collision voltage value for the conformer family in order to determine the main factors that drive the absolute deviations observed in CIU fingerprints. Our results indicate that nearly all of the albumin homologues tested access virtually identical unfolded conformer families, as defined by their centroid collision voltage and drift time values, when subjected to CIU. Critically, however, these same conformer families differ substantially in terms of their stability values. On the basis of this data, we draw two major conclusions: (1) The stabilities of CIU features are sensitive to small changes in protein primary structure. (2) The number of CIU features observed, centroid IM drift times, and activation voltage values are conserved across different protein homologues and are instead linked to native protein domain structure.

These results, therefore, indicate potential future applications for CIU in the context of structure predictions for large proteins of unknown folds based on CIU data, as well as high-throughput local stability measurements of domains within larger protein or multiprotein constructs. Furthermore, we anticipate future CIU-based separations of iso-mass, iso-CCS proteoforms for the purposes of protein identification and quantitation (Figure S5) based on the principles outlined in Figure 1.

Domain-Specific Chemical Probes for the Structural Interpretation of CIU Fingerprints. Our data linking the conformational families accessed by CIU and native protein domain structure motivated us to develop a mechanistic understanding of serum albumin unfolding in the gas phase. For this series of experiments, we chose to focus on the human variant of serum albumin (HSA), as it is arguably the most well studied and is supported by a large amount of crystallographic data associated with ligand binding.[35] Our approach involves correlating ligand dissociation energies with CIU features, where the binding location of the ligand is known from robust experimental data. First, we chose hemin as a marker for domain 1 (D1), as many data sets, including an X-ray structure, indicate a highly specific hemin binding site in this region for the HSA sequence.[35,36] Results from 15^+ ions (Figure 2) indicated that the hemin binding pocket on D1 is preserved through at least the first two CIU structural transitions we observe, and the ligand is finally dissociated from conformer family 3 as it begins to transition to family 4. Surprisingly, the third albumin domain, D3, positioned on the opposite end of the polypeptide chain from D1, shows similar results, indicating

DOI: 10.1021/jacs.6b11678
J. Am. Chem. Soc. 2017, 139, 534–540

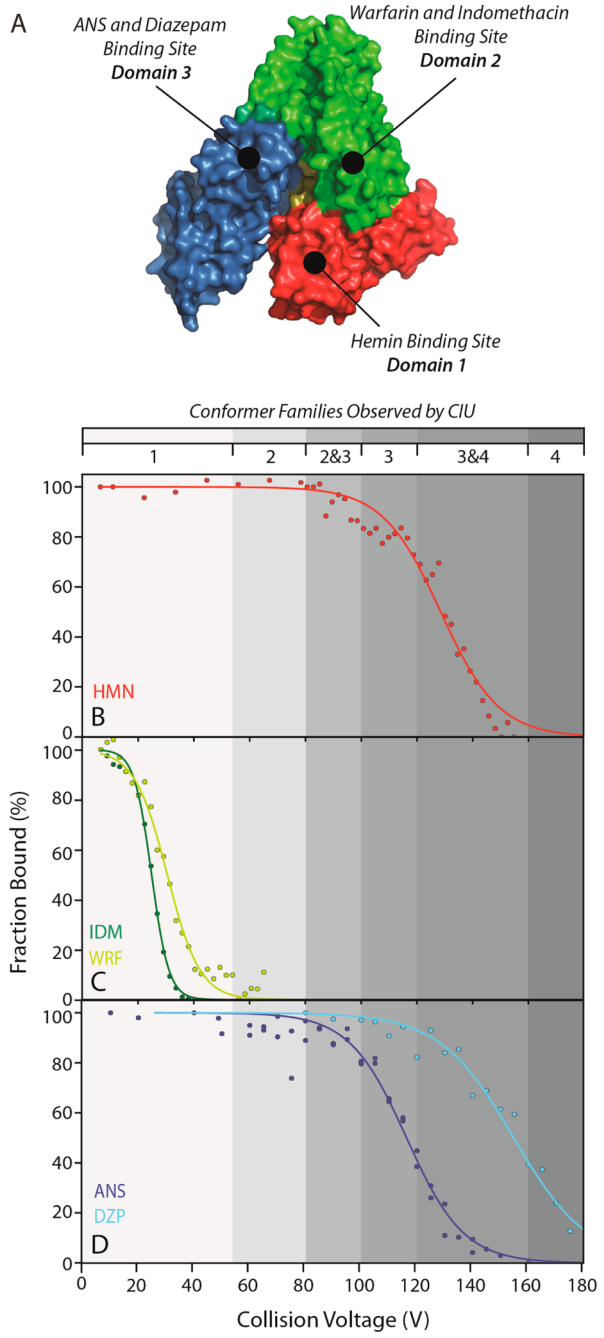

Figure 2. HSA domain-specific chemical probes of CIU. (A) Surface representation of HSA based on PDB ID 4K2C with ligand binding sites indicated. CID breakdown curves for HSA–ligand complexes, fitted to sigmoid functions. Data sets are shown for binders associated with domain 1 (B), 2 (C), and 3 (D). See text for abbreviation definitions. Overlaid on all plots is a color scale indicating the voltage ranges where different CIU conformer families are observed (see legend, top).

the preservation of the D3 drug binding site for both ANS[31] and diazepam[32,35] through the first two albumin conformer families observed. In contrast, ligands such as indomethacin and warfarin[1] that bind to a site on D2 are rapidly dissociated during the initial HSA CIU events observed at low collision voltages, despite similar overall binding affinities to the D1 and D3 binders described above. Of the ligands presented in Figure 2, we found no significant differences in the CIU fingerprints of ligand bound and apo species, with the exception of diazepam complexes, for which we observe large CID thresholds and stabilization of conformer family 3 (Figure S6). To validate these results, we examined the ligand dissociation behavior of hemin, warfarin, and diazepam from the 14^+ and 16^+ HSA ions (Figure S7). These data sets reinforced our hypotheses, as nearly identical behavior to the 15^+ ions described above was observed for 16^+ ions, and only minor deviations were detected in the 14^+ case. Additionally, we examined the behavior of two larger molecules, iodipamide[35] and thyroxine[37] (Figure S8) that are known to bind in two and four locations within the HSA structure, respectively. Data acquired for these ligands also support the hypothesis that the D2 binding site is affected early in collisional activation; however, structural interpretation of the CID data from these ligands proved to be difficult, as it was clear that both displayed evidence of significant cooperative stabilization (Figure S9).

In addition to the above-noted correlations between CID and CIU data, we interpret our HSA chemical probe data in the context of previous experiments correlating protein–ligand interactions with CID energies.[38−41] These early studies employing native ESI and CID demonstrated a strong correlation between the polar surface binding area of a ligand and the corresponding threshold collision energy required for ligand CID, although no similar correlation could be found for nonpolar binders (Figure S10). For each ligand in our study, we calculated the total polar surface area[42] as well as the total number of polar contacts for each albumin–ligand complex from available X-ray data sets.[43] We observe no correlation between our observed CID threshold energies for HSA–ligand complexes and any description of the native contacts formed between ligands and their respective protein binding pockets (Figure S10). This result, taken in context with the CIU/CID correlations observed in Figure 2, strongly indicates that the collisional ejection of a ligand from a multidomain protein system, such as HSA, is most strongly correlated with the structural cohesion of its resident domain, rather than the number of local contacts developed within a protein–ligand binding site.

Noncovalent Albumin Constructs Further Reveal the CIU Mechanism of HSA. To build on our understanding of the unfolding of HSA, we designed a series of CIU/CID experiments utilizing HSA constructs built as noncovalent complexes comprised of individual HSA domains (Figures S11–S19). First, we incubated covalently attached albumin domains 1 and 2 (D12) with D3 to generate a noncovalent dimer that mimics full length HSA (D12–D3). These results were compared with nonspecific dimers where D3 was replaced with either D1 or D2, creating D12–D1 and D12–D2, respectively. Surprisingly, we were able to generate stable, noncovalent albumin mimics that had ground state drift time values nearly identical to their covalently bound, native counterparts. CID analysis of these complexes (Figure 3A) revealed that the two mismatched dimers showed nearly identical CID behavior, both possessing increased stability relative to D12–D3. Specifically, D12–D1 and D12–D2 begin to dissociate at around 80 V, similar to D12–D3; however, neither achieves the expected sigmoidal trend between intact dimer intensity and collision voltage, and instead both proceed to dissociate along an apparently frustrated, near-linear trend-line. A comparison of the CIU fingerprints for these mismatched dimers (Figure S20) reveals that D12–D1 and D12–D2 are unable to access CIU conformer family 3, which

DOI: 10.1021/jacs.6b11678
J. Am. Chem. Soc. 2017, 139, 534–540

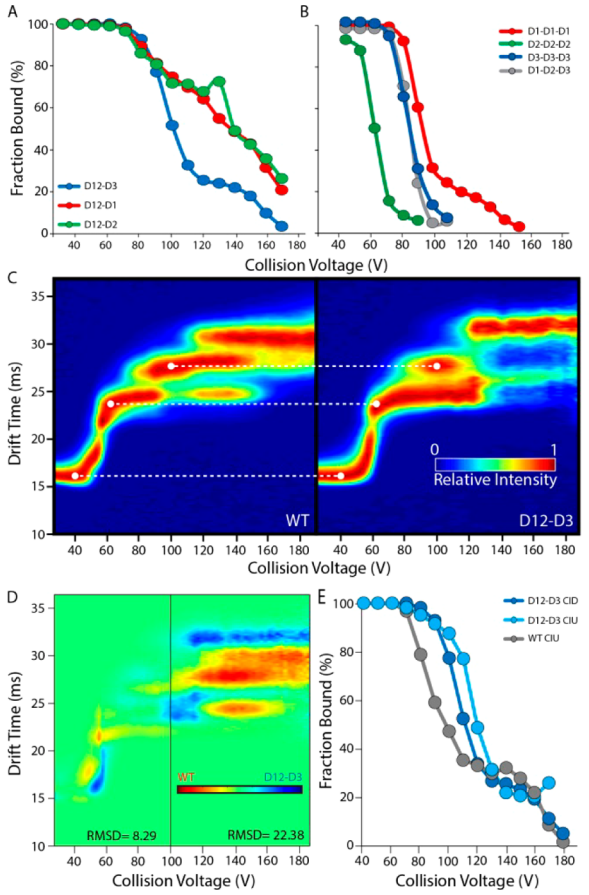

Figure 3. CIU/CID analysis of 15^{+} noncovalent, reconstituted albumins. (A) CID breakdown curves representing the dissociation of a noncovalently bound D3 domain from the covalent D12 fusion protein. (B) CID breakdown curves representing the dissociation of a noncovalent subunit from a noncovalent homotrimer of albumin domains. (C) CIU comparison of WT HSA with the noncovalent D12−D3 construct. Dashed lines indicate strong correlation between the first three CIU features observed. (D) CIU difference plot between WT and D12−D3 HSA. RMSD values are calculated for before and after the transition to nonsigmoidal CID behavior (black line). (E) Correlation between the structural transition from CIU conformer 2 to 3 and the CID behavior of D12−D3.

we find is necessary for the efficient dissociation of D3 from the D12−D3 dimer. Next, we used individual HSA domains to construct both all the possible homotrimers and a heterotrimer of native-like composition for CIU and CID analysis. CID data shown in Figure 3B illustrates that homotrimers constructed entirely from D2 are the least stable, and those comprised of D1 are the most stable, with D3 and D1−D2−D3 trimers presenting intermediate, and nearly identical, stabilities (Figure 3E).

Figure 3C compares the CIU fingerprint for native-like HSA (left) with the D12−D3 construct (right) discussed above. We find a striking correlation in the positions of CIU features and transitions for these two constructs at collision voltages lower than the CID threshold for D3 ejection from the D12−D3 dimer. In order to quantify the similarity of the CIU data shown in Figure 3C, we computed two RMSD values from the data sets: one for all CIU data collected at collision voltages less than 100 V (at which CID has depleted D12−D3 by 50%) and another for all CIU data collected above that value (Figure 3D). Aside from some additional stability imparted in the non-covalent complex, a difference analysis shows that these fingerprints are nearly identical at lower collision voltages, as evidenced by a relatively low CIU RMSD value of 8.29. In contrast, the RMSD value computed for CIU data acquired above 100 V is 22.28, strongly indicating that D12−D3 can neither efficiently access conformer family 3 nor any of conformer family 4. Instead, D12−D3 appears to access a new final unfolded state for CIU/CID above 100 V. Surprisingly, CIU fingerprints of both D1 and D3 homotrimers, as well as for the D1−D2−D3 heterotrimer, showed similar levels of correlation with native HSA CIU prior to their respective CID thresholds (Figure S21). In Figure 3E, we compare the transition from conformer family 2 to 3 in both native and D12−D3 albumins with the CID breakdown curve that tracks D3 ejection from the D12−D3 dimer. The same nonsigmoidal trends are observed in all three data sets, indicating a mechanistic connection between the appearance of CIU conformer family 3 in both WT HSA and D12−D3, as well as the ejection of D3 from D12−D3. We observe an average charge state for dissociated D3 of $\sim 8^{+}$, which amounts to 53% of the parent ion charge, thus strongly indicating D3 is unfolded prior to ejection from the D12−D3 complex.[44]

Mechanism of Gas-Phase Albumin Unfolding. Taken together, our data allows us to generate the first detailed unfolding model for a solvent-free multidomain protein. Our chemical probe studies indicate that ligands bound to D2 generally dissociate iso-energetically with the transition from conformer family 1 to 2, leading us to assign CIU conformer family 2 to a D2 unfolding event. Supporting this assignment is our CID/CIU data for D2 noncovalent trimer ions, indicating that D2 forms the least stable homotrimer out of all those studied here. Next, our CID data for D12−D3 inform our assignment of CIU conformer family 3 as related to unfolding of D3. Interestingly, our ligand binding studies indicate that D3-bound ligands can survive activation past this transition despite relying upon a relatively low number of polar contacts to remain within the D3 binding site. Taking this into account, we assign this transition to the partial unfolding of D3 in a manner that leaves its diazepam binding site intact. Finally, on the basis of both the large stabilities of D1-based constructs and D1/D3 chemical probe data, we assign CIU conformer family 4 to a coupled unfolding event involving both D1 and the remainder of D3.

By combining WT HSA CIU data with CID data from D12−D3, we can also infer a role for charge migration in the unfolding of large multidomain proteins. The dissociation products of D12−D3 are those expected from multiprotein CID: highly charged, unfolded D3, and charge stripped, compact D12.[44] Although such results have been observed in CID data for many multiprotein complexes, the finding takes on new meaning in the context of understanding the CIU of a single protein chain. Considering the remarkable similarities between the measured unfolding data for HSA and D12−D3, we argue that the CIU of WT HSA must involve asymmetric charge migration during the first unfolding steps, and that the charge is likely redistributed evenly across newly revealed protein surfaces as unfolding continues.

■ CONCLUSIONS

This work presents the most thorough investigation to date of the gas-phase unfolding of a multidomain protein. While the scope of our study is limited to albumins, a careful analysis of our data indicates trends that may be generalizable across many

DOI: 10.1021/jacs.6b11678
J. Am. Chem. Soc. 2017, 139, 534−540

classes of proteins and protein complexes. Our results indicate the sensitivity of CIU experiments to subtle changes in primary structure, where the tertiary structure remains essentially unchanged. Stated more specifically, we show that the conformational intermediates accessed during unfolding are dictated entirely by the tertiary structure of the protein, whereas the stability of those intermediates is determined by the underlying primary structure.

In addition to the insights above, our data set reveals previously unknown correlations between gas-phase protein dissociation and unfolding. For example, our data show a clear correlation between the CIU of individual domains within a protein and the threshold voltage associated with CID-based ligand ejection. Interestingly, we did not find any correlation between our CID data and ligand−protein polar contacts/surface areas, in contrast to previous literature for smaller, single-domain protein systems. Additionally, a comparison of our CIU and CID data from noncovalent models of HSA strongly indicates that surface charges are redistributed during the CIU of multidomain proteins, similar to the mechanism proposed to describe multiprotein CID.[44]

A comparison of the mechanism shown in Figure 4 with previously reported solution-phase measurements[32,35−37] indicates key similarities between solvent-free and solvated albumin unfolding. Guanidine hydrochloride-based denaturation of albumin bound to many of the probes used in our studies has identified the unfolding of D3 as a relatively early participant in the overall albumin unfolding process, and D1 has the most stable albumin domain. Additionally, these studies describe a modular, domain-centric unfolding pathway for albumin in solution, in agreement with our gas-phase studies. In contrast, solution-phase studies do not capture large conformational shifts, like those that we attribute to D2 unfolding. While it is not surprising that gas-phase CIU does not precisely mimic protein denaturation in solution, the level of correlation that we observe projects a tantalizing future for CIU measurements in understanding the fundamental forces that drive native protein stability and predicting domain organization.

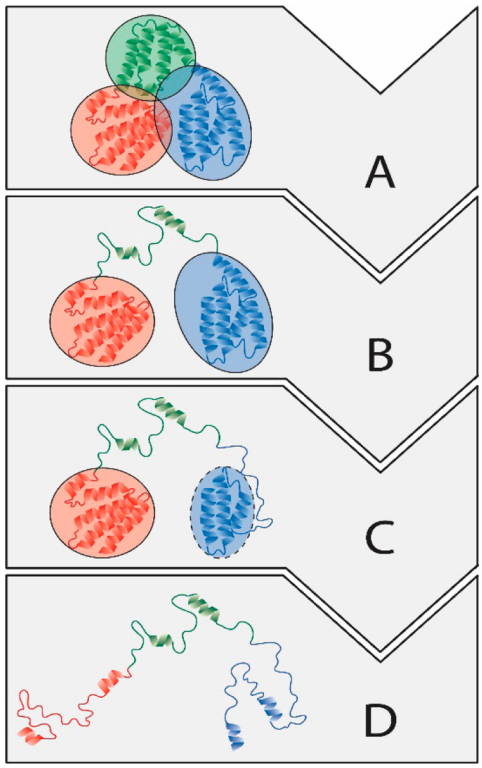

Figure 4. A modular unfolding mechanism for 15^+ human serum albumin. Proposed structural transitions that agree with experimental evidence are depicted in a cartoon. Domains are indicated in red for D1, green for D2, and blue for D3. (A) Albumin compacts upon entry to the gas phase, and all three domains are in a native-like conformation (represented by circles). (B) As ion energy is increased, D2 undergoes unfolding, leaving the other two domains in a relatively native-like state. (C) Partial unfolding of D3 (indicated by the dashed ellipse) is achieved only at higher ion energies. (D) At the highest ion energies accessed in our experiment, all native-like protein structure is lost, including D1.

Although the experimental data presented in this report provides our most detailed insights into gas-phase protein unfolding to date, the resolution of our model is certainly limited. In order to improve our understanding of both CIU and protein structure in general, it is clear that improvements in both gas-phase molecular dynamics simulations and experimental IM-MS techniques will be required. For example, tandem IM technologies,[45] capable of both assessing the direct connectivity between CIU conformer families and revealing the fine structure within such families, will undoubtedly prove useful in achieving CIU models of greater detail than shown here. In addition, the synergy between CIU data sets and recent advancements that combine charge migration algorithms with atomistic molecular dynamics simulations of large proteins[46] is clear. Future efforts in both theory and experiment will likely build on the insights discussed here, along with accumulated CCS data from these studies (Tables S7 and S8), in order to move our understanding of solvent-free protein folding forward, acquire structural data for refractory regions of the proteome, and access canonically challenging targets for the discovery of next-generation therapeutics.

■ ASSOCIATED CONTENT

Supporting Information

The Supporting Information is available free of charge on the ACS Publications website at DOI: 10.1021/jacs.6b11678.

Raw IM-MS data, CIU and CID data, collision cross sections, ligand binding, and sequence analysis (PDF)

■ AUTHOR INFORMATION

Corresponding Author

*bruotolo@umich.edu

ORCID

Brandon T. Ruotolo: 0000-0002-6084-2328

Notes

The authors declare no competing financial interest.

■ ACKNOWLEDGMENTS

The authors would like to thank the National Institutes of Health (NIGMS, GM095832) and the University of Michigan Department of Chemistry for their support. J.D.E. also acknowledges support from the University of Michigan Rackham Graduate School in the form of a Research Award. Additionally, we thank Prof. Robert Kennedy for his help with preparing diazepam treated albumin samples for CIU analysis.

DOI: 10.1021/jacs.6b11678
J. Am. Chem. Soc. 2017, 139, 534−540

REFERENCES

(1) Metallo, S. J. *Curr. Opin. Chem. Biol.* **2010**, *14*, 481.
(2) Dill, K. A.; MacCallum, J. L. *Science* **2012**, *338*, 1042.
(3) Zhang, Y. *BMC Bioinf.* **2008**, *9*, 40.
(4) Berman, H. M.; Kleywegt, G. J.; Nakamura, H.; Markley, J. L. *Structure* **2012**, *20*, 391.
(5) Ward, A. B.; Sali, A.; Wilson, I. A. *Science* **2013**, *339*, 913.
(6) Fenn, J. B.; Mann, M.; Meng, C. K.; Wong, S. F.; Whitehouse, C. M. *Science* **1989**, *246*, 64.
(7) Tanaka, K.; Waki, H.; Ido, Y.; Akita, S.; Yoshida, Y.; Yoshida, T. *Rapid Commun. Mass Spectrom.* **1988**, *2*, 151.
(8) Karas, M.; Hillenkamp, F. *Anal. Chem.* **1988**, *60*, 2299.
(9) Benesch, J. L. P.; Ruotolo, B. T.; Simmons, D. A.; Robinson, C. V. *Chem. Rev.* **2007**, *107*, 3544.
(10) Xie, Y. M.; Zhang, J.; Yin, S.; Loo, J. A. *J. Am. Chem. Soc.* **2006**, *128*, 14432.
(11) Liu, L.; Bagal, D.; Kitova, E. N.; Schnier, P. D.; Klassen, J. S. *J. Am. Chem. Soc.* **2009**, *131*, 15980.
(12) Wyttenbach, T.; Bowers, M. T. *J. Phys. Chem. B* **2011**, *115*, 12266.
(13) Pierson, N. A.; Chen, L.; Valentine, S. J.; Russell, D. H.; Clemmer, D. E. *J. Am. Chem. Soc.* **2011**, *133*, 13810.
(14) Wood, T. D.; Chorush, R. A.; Wampler, F. M.; Little, D. P.; O'Conner, P. B.; McLafferty, F. W. *Proc. Natl. Acad. Sci. U. S. A.* **1995**, *92*, 2451.
(15) Valentine, S. J.; Clemmer, D. E. *J. Am. Chem. Soc.* **1997**, *119*, 3558.
(16) Oomens, J.; Polfer, N.; Moore, D. T.; van der Meer, L.; Marshall, A. G.; Eyler, J. R.; Meijer, G.; von Helden, G. *Phys. Chem. Chem. Phys.* **2005**, *7*, 1345.
(17) Wyttenbach, T.; von Helden, G.; Bowers, M. T. *J. Am. Chem. Soc.* **1996**, *118*, 8355.
(18) Wolynes, P. G. *Proc. Natl. Acad. Sci. U. S. A.* **1995**, *92*, 2426.
(19) Ruotolo, B. T.; Robinson, C. V. *Curr. Opin. Chem. Biol.* **2006**, *10*, 402.
(20) Niu, S.; Rabuck, J. N.; Ruotolo, B. T. *Curr. Opin. Chem. Biol.* **2013**, *17*, 809.
(21) Mayer, P. M.; Martineau, E. *Phys. Chem. Chem. Phys.* **2011**, *13*, 5178−5186.
(22) Shelimov, K. B.; Clemmer, D. E.; Hudgins, R. R.; Jarrold, M. F. *J. Am. Chem. Soc.* **1997**, *119*, 2240.
(23) Ruotolo, B. T.; Hyung, S.-J.; Robinson, P. M.; Giles, K.; Bateman, R. H.; Robinson, C. V. *Angew. Chem., Int. Ed.* **2007**, *46*, 8001.
(24) Hopper, J. T. S.; Oldham, N. J. *J. Am. Soc. Mass Spectrom.* **2009**, *20*, 1851.
(25) Hyung, S.-J.; Robinson, C. V.; Ruotolo, B. T. *Chem. Biol.* **2009**, *16*, 382.
(26) Han, L.; Hyung, S.-J.; Mayers, J. J. S.; Ruotolo, B. T. *J. Am. Chem. Soc.* **2011**, *133*, 11358.
(27) Zhou, M.; Dagan, S.; Wysocki, V. H. *Analyst* **2013**, *138*, 1353.
(28) Rabuck, J. N.; Hyung, S.-J.; Ko, K. S.; Fox, C. C.; Soellner, M. B.; Ruotolo, B. T. *Anal. Chem.* **2013**, *85*, 6995.
(29) Niu, S.; Ruotolo, B. T. *Protein Sci.* **2015**, *24*, 1272.
(30) Tian, Y.; Han, L.; Buckner, A. C.; Ruotolo, B. T. *Anal. Chem.* **2015**, *87*, 11509.
(31) Zhong, Y.; Han, L.; Ruotolo, B. T. *Angew. Chem.* **2014**, *126*, 9363.
(32) Ahmad, B.; Ahmed, M. Z.; Haq, S. K.; Khan, R. H. *Biochim. Biophys. Acta, Proteins Proteomics* **2005**, *1750*, 93.
(33) Ruotolo, B. T.; Benesch, J. L.; Sandercock, A. M.; Hyung, S.-J.; Robinson, C. V. *Nat. Protoc.* **2008**, *3*, 1139.
(34) Eschweiler, J. D.; Rabuck-Gibbons, J. N.; Tian, Y.; Ruotolo, B. T. *Anal. Chem.* **2015**, *87*, 11516.
(35) Ghuman, J.; Zunszain, P. A.; Petitpas, I.; Bhattacharya, A. A.; Otagiri, M.; Curry, S. *J. Mol. Biol.* **2005**, *353*, 38.
(36) Zunszain, P. A.; Ghuman, J.; Komatsu, T.; Tsuchida, E.; Curry, S. *BMC Struct. Biol.* **2003**, *3*, 6.
(37) Petitpas, I.; Petersen, C. E.; Ha, C.-E.; Bhattacharya, A. A.; Zunszain, P. A.; Ghuman, J.; Bhagavan, N. V.; Curry, S. *Proc. Natl. Acad. Sci. U. S. A.* **2003**, *100*, 6440.
(38) Wu, Q.; Gao, J.; Joseph-McCarthy, D.; Sigal, G. B.; Bruce, J. E.; Whitesides, G. M.; Smith, R. D. *J. Am. Chem. Soc.* **1997**, *119*, 1157.
(39) Rogniaux, H.; Van Dorsselaer, A.; Barth, P.; Biellmann, J. F.; Barbanton, J.; van Zandt, M.; Chevrier, B.; Howard, E.; Mitschler, A.; Potier, N.; Urzhumtseva, L.; Moras, D.; Podjarny, A. *J. Am. Soc. Mass Spectrom.* **1999**, *10*, 635.
(40) El-Kabbani, O.; Rogniaux, H.; Barth, P.; Chung, R. P. T.; Fletcher, E. V.; Van Dorsselaer, A.; Podjarny, A. *Proteins: Struct., Funct., Genet.* **2000**, *41*, 407.
(41) Stojko, J.; Fieulaine, S.; Petiot-Becard, S.; Van Dorsselaer, A.; Meinnel, T.; Giglione, C.; Cianferani, S. *Analyst* **2015**, *140*, 7234.
(42) Ertl, P.; Rohde, B.; Selzer, P. *J. Med. Chem.* **2000**, *43*, 3714.
(43) Wallace, A. C.; Laskowski, R. A.; Thornton, J. M. *Protein Eng., Des. Sel.* **1995**, *8*, 127.
(44) Hyung, S.-J.; Ruotolo, B. T. *Proteomics* **2012**, *12*, 1547.
(45) Koeniger, S. L.; Merenbloom, S. I.; Valentine, S. J.; Jarrold, M. F.; Udsth, H. R.; Smith, R. D.; Clemmer, D. E. *Anal. Chem.* **2006**, *78*, 4161.
(46) McAllister, R. G.; Metwally, H.; Sun, Y.; Konermann, L. *J. Am. Chem. Soc.* **2015**, *137*, 12667.

DOI: 10.1021/jacs.6b11678
J. Am. Chem. Soc. 2017, 139, 534−540